SSR Journal of Multidisciplinary (SSRJM)

Volume 3, Issue 2, 2026 Homepage: https://ssrpublisher.com/ssrjm/
Email: office.ssrpublisher@gmail.com

OPEN ACCESS

ISSN: 3049-1304

Scaps-1D Simulation, Effect of Device Architecture and Performance Analysis of $C_sP_bI_3$ Inorganic Perovskite Solar Cell Material

Julius Felix, Akpa Victor Ogbonnaya & Salaudeen Olaiya Abdulwasiu

Department of Physics, University of Abuja, Abuja Nigeria

Received: *11.01.2026* | ***Accepted:*** *30.01.2026* | ***Published:*** *01.02.2026*

***Corresponding Author:** Julius Felix

DOI: *10.5281/zenodo.18449157*

Abstract **Original Research Article**

PSC device is one of the evolving solar renewable energy resources that is globally best accepted for the replacement of conventional CIGS energy resources because it is efficient and profound for energy generation. Ensuring the effectiveness of this device is crucial, which will ensure its efficiency during conversion. In this research $CsPbI_3$ inorganic material was numerically simulated using the SCAPS-1D software with initial result of PCE, FF, J_{sc} and V_{oc} obtained as 31.61 %, 86.88 %, 42.0857 mA/cm^2, and 0.865 V respectively. The effect of values on HTL, absorber layer and ETL simulated the results shows that the thickness of each layer plays a vital role on the optimization of PSC devices except for HTL where only a little parameter changes are observed. Nevertheless, the acceptor density variation on HTL shows a unique increased effect on the PSC structure performance with a very good desirable optimized values of PCE, Jsc and Voc which was observed as 31.7 %, 86.9 %, 42.1 mA/cm^2, and 0.993 V at 10^{20} cm^{-3}. This shows that the choice of parameters for the fabrication of a PSC device is important, because it will determine the effectiveness of the device.

Keywords: CsPbI3, PSC, SCAPS-1D Simulation.

1. Introduction

Energy crisis occurs as a result of limited resources, materials, and infrastructure which is generally observed across the globe, in Africa it has become very alarming where the energy supply do not meet the demand despite having the most abundant renewable energy resources (solar) present which is clean with no noise and minimal requirement of sophisticated equipment for harvest [1, 2]. The energy obtained from solar radiation is enough to solve the energy crisis observed across the globe but the materials available for harvesting this energy those not meet the requirement, compared to what the sun is generating daily, the power conversion efficiency (PCE) of solar energy harvesters especially the solar cell materials is minimal which has been reported to be around ~25% [3]. Improving the performance of solar cells for energy conversion has been of concern to researchers because energy obtained from the sun remains the best solution that will solve the increasing global demand of energy [4]. Although there is a significant improvement in recent years where thin film nanoparticles such as CIGS solar cell and now the Perovskite Solar cell (PSC) in organic or inorganic form has been fabricated for solar energy harvest [5]. So far, the

performance of this photovoltaic cell, which was fabricated recently and is found in the market, has been highly recommendable due to its improved properties, nevertheless there is still more to do because the energy conversion efficiency is not even half way yet compared to what the sun is generating daily [6] Therefore it is necessary to consider improving the properties of this PSC, this will show a significant shift in the energy industry toward enabling an improved performance of solar cells for energy generation [1].

1.1.Perovskite Solar Cell (PSC)

Perovskite Solar cell is currently the most significant material for photovoltaic energy harvest replacing CIGS solar cells, it is less toxic with low production cost and flexible for placement on substrate. PSC remains the best PV with Power conversion Efficiency (PCE), but it is limited to the expectation of achieving absolute PCE with longevity of PV cells. This weakness observable in PSC is due to the type of material used during fabrication such as $CsPbCl_3$, $CsPbI_3$, $CsSnI_3$, $CsSnGeI_3$, $Cs_3Bi_2I_9$, $MASnI_3$, $CH_3NH_3SnI_3$, $CH_3NH_3PbI_3$, among others. The crystallinity of the nanoparticle also affects the performance of PV modules, because pure crystals are said to provide excellent optical properties for PV cells to enable efficient energy conversion, the thickness and the doping concentration of the nanostructures are also included in this case. Similarly the performance of PSC is been affected by the different layers of its structure which include the Hole transport layer (HTL), Electron Transport layer(ETL), the Energy Gab (Eg), the temperature and the mobility of the nano-pico-particles etcetera [1]. These parameters influence the properties of these particles for energy conversion in solar cells, and the effect is significantly observed in the Field Factor (FF), Quantum Efficiency of the PSC (QE) and PCE (%) analysis obtained from the I-V and QE characteristics curve.

1.2. In-organic $C_sP_bI_3$ PSC Material

Cesium Lead Iodide ($CsPbI_3$) is an In-organic halide PSC material highly considered for the fabrication of PV cells, it is one of the best recent PSC material that has drawn many researchers attention because of it remarkable improved optical and electrical properties and its effect is observed on PCE, FF and QE. Among other PSC materials, $CsPbI_3$ is said to be polymorphs in nature with different vibrational thermodynamic properties, its UV-Vis absorption properties shows a unique shift from what was already obtainable which makes it one of the most promising materials for solar energy conversion.

Boussaada (2025) reported an ETL and photovoltaic analysis using 1D-SCAPS simulation of $CsPbI_3$ materials, during the optimization simulation of the material with thickness of 900nm for the absorber layer, doping level of 1.5 X 10^{15} cm^{-3}, and a defect density of 1 x $10^{12}cm^{-3}$, the PSC simulation result parameters was reported with the following data: FF 82.43%, J_{sc} 20.32mA/cm^2 and a PCE of 21.34%. This shows a highly improved performance compared to the experimental data [1]. Comparing with the result obtained by Goje (2023) in the optimization of Al_2O_3 material ETL layer with thickness of 40nm, the FF changes from 68.11% , Jsc of 37.23mA/cm^2 with PCE of 20.61% at 300K, this shows the $CsPbI_3$ is more significant and better compared to Al_2O_3 [7]. The HTL impact in $CsSnI_3$ inorganic material reported by Adnan (2022) shows a remarkable shift from the previously reported research with simulation parameters of 86.6% FF, 33.5mA/cm^2 Jsc and 28.76% PCE, with absorber thickness of 0.6µm [8]. Furthermore, Danladi (2022) conducted a research using the SCAPS software on the thickness variation of $CH_3NH_3SnI_3$ inorganic material from 100-1300nm at 300K, the result indicate a FF of 53.439%, Jsc of 21.166mA/cm2, Voc of 0.741 and PCE of 8.382% [9].

In this research, 1D-SCAPS simulation tool will be deployed to optimize Perovskite Solar Cell Using Inorganic $CsPbI_3$ material.

2. Device Simulation

Improving the optical and electrical properties of perovskite solar cell (PSC) is not best to be first considered experimentally, rather simulation of PSC properties is paramount to obtaining the best data required for the fabrication of PSC. The 1D SCAPS simulation tool version 3.1.10, developed at the University of Gen, department of Electronics and Information Systems (ELIS)

Campus Ardoyen, Technologiepark 914, Grote Steenweg Noord 9052 Gent-Zwijnaarde Belgium by Marc Burgelman, Koen Decock, Alex Niemegeers, Johan Verschraegen, and Stefaan Degrave. The simulation of the PSC data in SCAPS is achieved by solving the Poisson's and Continuity Equations which was developed to solve the relationship between the electric field of P-N Junction and space charge density [10].

2.1. Device Structure and Inputs Parameters

The light spectrum of AM1_5G 1 at 300K temperature value was used for the stimulation as displayed in figure 2.1 (Action panel) with a constant illumination of 1000W/m^2. The Action panel enables selection of I-V and QE properties to be analyzed in order to get the desirable result.

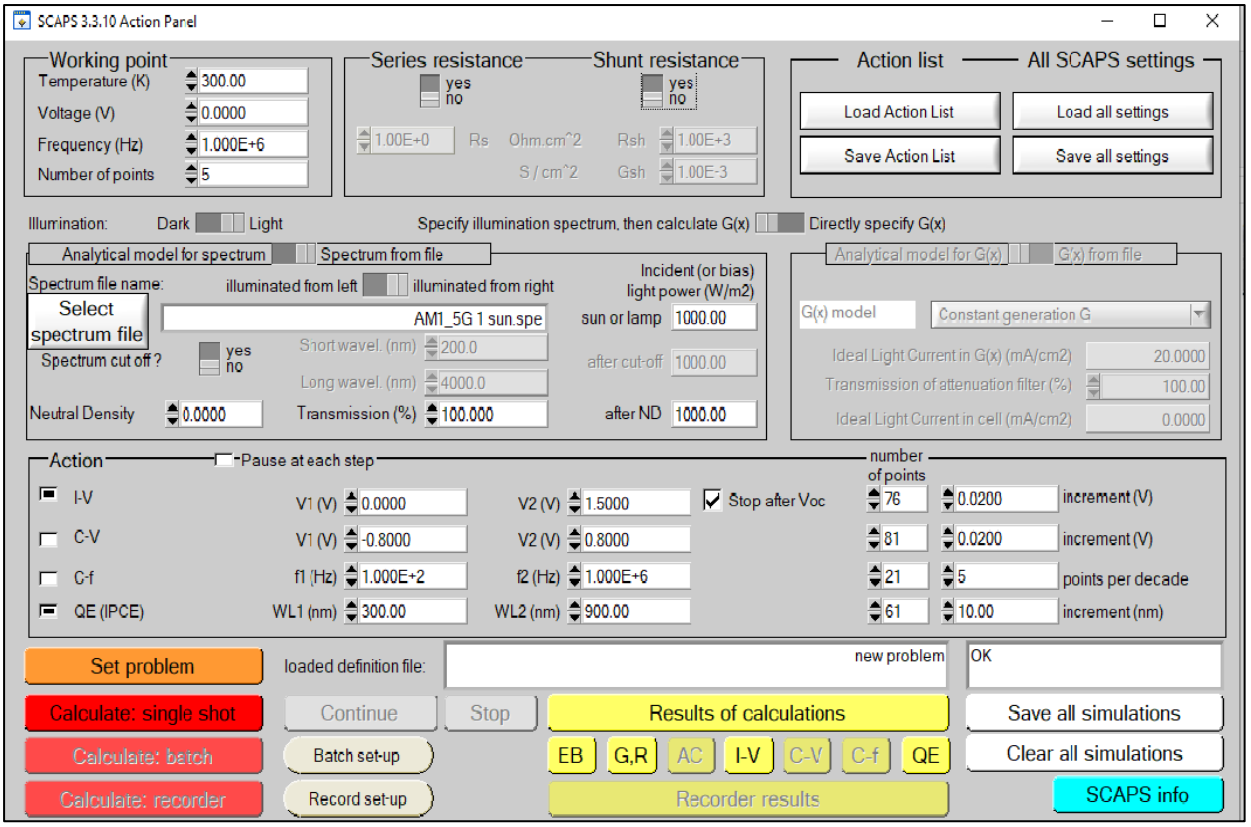

Figure 2.1 Device Launching Properties

Figure 2.2 shows the SCAPS configuration of the PSC in the form of FTO_TiO_2_$CsPbI_3$_Spiro-OMeTAD. The FTO represents the front contact, TiO_2 the ETL layer while the Absorber layer (ABL) was inculcated with $CsPbI_3$ elemental structure and the Spiro-OMeTAD was used as the HTL layer.

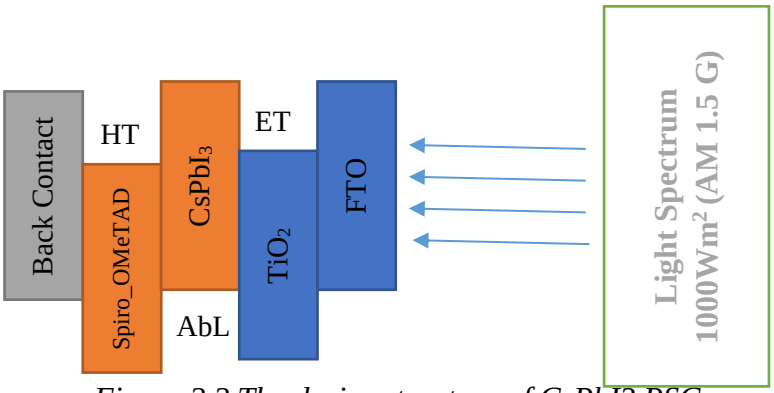

Figure 2.2 The device structure of CsPbI3 PSC

The necessary input parameters for all the structure layers are shown in Table 2.1, this include the thickness, electron affinity, band gab, dielectric permittivity, effective density, thermal velocity, mobility, and Donor and Acceptor densities while Table 2.2 shows the interface defect parameters which include Defect type, Electron capture cross section (cm^2), Holes capture cross section (cm^2), Energy distribution, and Energy with respect to reference (eV) [11].

Table 2.1 SCAPS Device input parameters for the simulation of PSC structure

Properties	*$CsPbI_3$*	*TiO_2*	*FTO*	*Spiro_OMeTAD*
Thickness (µm)	0.8	0.01	0.1	3.0
Band Gab Eg (eV)	1.1	2.5	2.5	1.2
Electron Affinity x (eV)	4.5	4.5	4.6	4.6
Dielectric Permittivity ε_r	10	10	10	6
CB Effective Density State N_c ($1/cm^3$)	1×10^{19}	1×10^{18}	1×10^{18}	1×10^{18}
VB Effective Density State N_v ($1/cm^3$)	1×10^{19}	1×10^{19}	1×10^{19}	1×10^{19}
Electron Thermal Velocity (cm/s)	1×10^{7}	1×10^{7}	1×10^{7}	1×10^{7}
Hole Thermal Velocity (cm/s)	1×10^{7}	1×10^{7}	1×10^{7}	1×10^{7}
Electron mobility μ_n (cm^2/Vs)	50	50	50	50
Hole mobility μ_p (cm^2/Vs)	50	50	50	50
Donor density (ND) $1/cm^3$	-	1×10^{12}	1×10^{19}	-
Acceptor density (NA) $1/cm^3$	1×10^{19}	1×10^{15}	-	1×10^{22}

Radiative recombination (cm^3/s)	0	1×10^{-15}	0	1×10^{-12}
Auger electron capture (cm^6/s)	2×10^{-31}	0	0	1×10^{-29}
Auger hole capture (cm^6/s)	1×10^{-32}	1×10^{-33}	0	1×10^{-29}
Defect density (cm^{-3})	1×10^{14} 1×10^{12}	1×10^{14}	1×10^{14}	1×10^{13} 1×10^{14}

Table 2.2 Interface defect input parameters

Parameters	*Spiro_OMeTAD/$CsPbI_3$*	*$CsPsI_3/TiO_2$*	*TiO_2/FTO*
Defect type	Acceptor	Donor	Donor
Electron capture cross section (cm^2)	1×10^{-18}	1×10^{-19}	1×10^{-16}
Holes capture cross section (cm^2)	1×10^{-19}	1×10^{-18}	1×10^{-19}
Energy distribution	Single	single	single
Energy with respect to reference (eV)	0.9	0.7	0.3
Total density (cm^{-3})	1×10^{10}	1×10^{9}	1×10^{10}

3. Results and Discussion

Experimental values are essential towards ensuring optimal simulation data analysis and interpretation for improving device performance, knowing the correct parameters needed for the fabrication of PSC devices support advancement and durability.

3.1 Initial Device Data Analysis

The initial simulation data gives the current-density and voltage plot, quantum efficiency with wavelength/photon energy, and the device energy band profile as shown in figure 3.1

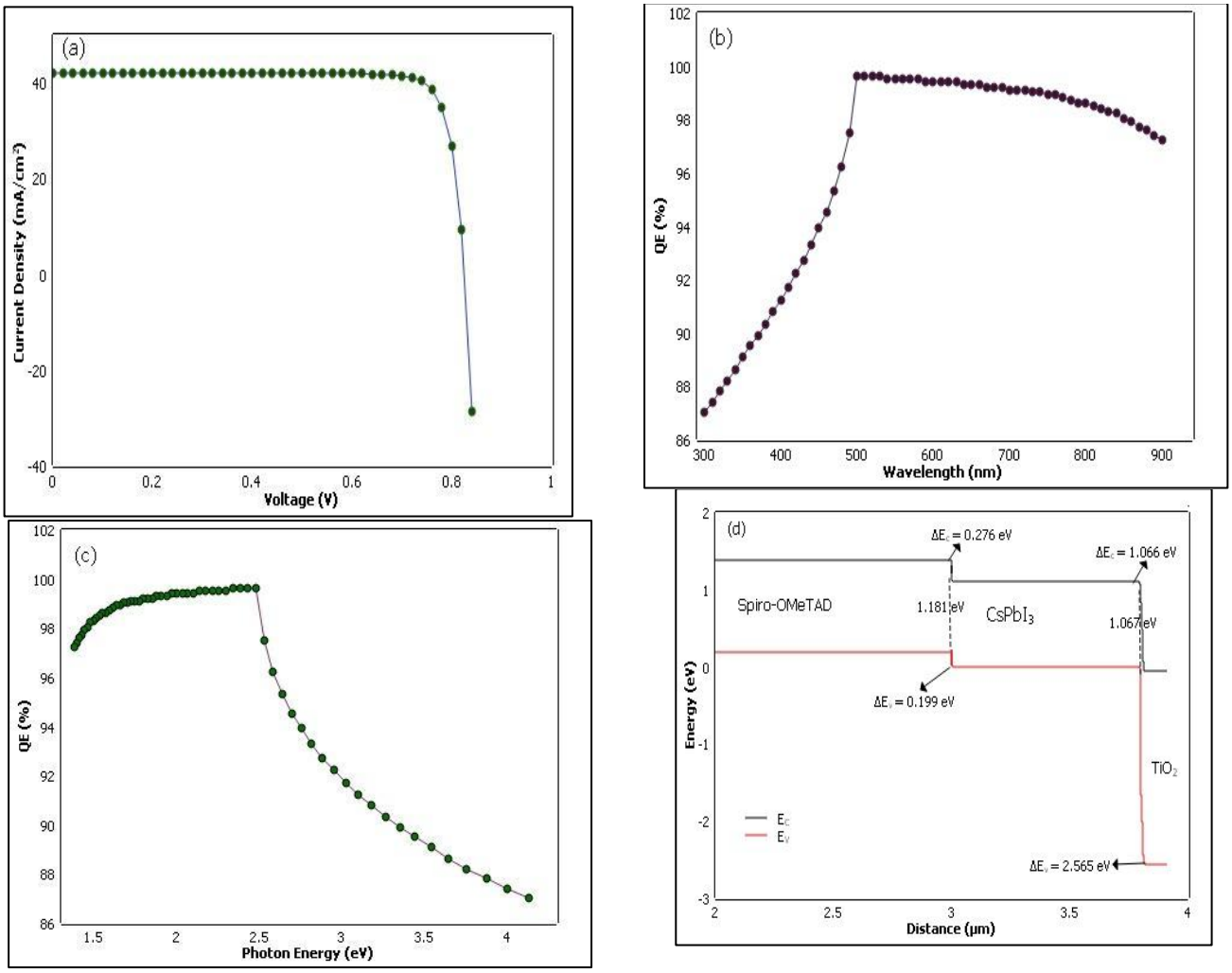

Figure 3.1 Initial simulation characteristics of (a) current density and voltage (b) QE and wavelength (c) QE and Photon energy and (d) the energy band profile display

The first simulation was carried out under light mode illumination with result of Short Circuit Current (J_{sc}) 42.0857 (mA/cm^2), Fill Factor (FF) 86.88 %, and Power Conversion Efficiency (PCE) of 31.61 % with an Open Circuit Voltage (V_{oc}) of 0.865V. this result is similarly to what was obtained in [2], [12]and [13] in agreement with the result obtained in [14] and [3], the result in this research shows a slide improvement to the experimental results this is as a result of the addition of some parameters such as the doping concentration, radiative recombination coefficient, Auger electron/hole capture coefficient and the interface parameters. Figure 3.1b and 3.1c shows the plot of QE against wavelength and photon energy, the wavelength ranged from 300-900 nm and has attained a maximum value of 99.66 % at 499.8 nm, the QE rises from 87.01 % at 799.5 nm to attain that maximum which indicates the coverage of the entire visible region and reaches a good absorption maximum before declining to 900 nm [15]. Figure 3.1d shows the energy gap of the Spiro-OMeTAD/$CsPbI_3$/TiO_2/FTO structure with 0.199 eV and 0.276 eV at Spiro-OMeTAD/$CsPbI_3$ interface, and at $CsPbI_3$/TiO_2 interface it was 2.565 eV and 1.066 eV, this is important because it will help improve the flow of charge careers at the interface which is required for enhance perovskite solar cells [16].

3.2 HTL layer thickness effect on the performances of PSC

The thickness of each layer of the PSC plays a significant role on the performance of the solar device, for HTL layer thickness as observed from the stimulation data shown in Table 3.1 and

figure 3.2 were observed at 1-10 µm which result to different values of PCE, FF, Voc and Jsc.

Table 3.1 I-V curve Simulation parameters with varying thickness

Thickness (µm)	PCE (%)	FF (%)	V_{oc} (V)	J_{sc} (mA/cm^2)
1	31.6	86.9	0.865	42.1
2	31.6	86.9	0.865	42.1
3	31.6	86.9	0.865	42.1
4	31.6	86.9	0.865	42.1
5	31.6	86.9	0.865	42.1
6	31.6	86.9	0.865	42.1
7	31.6	86.9	0.865	42.1
8	31.6	86.9	0.865	42.1
9	31.4	83.4	0.900	42.1
10	30.6	75.6	0.993	42.1

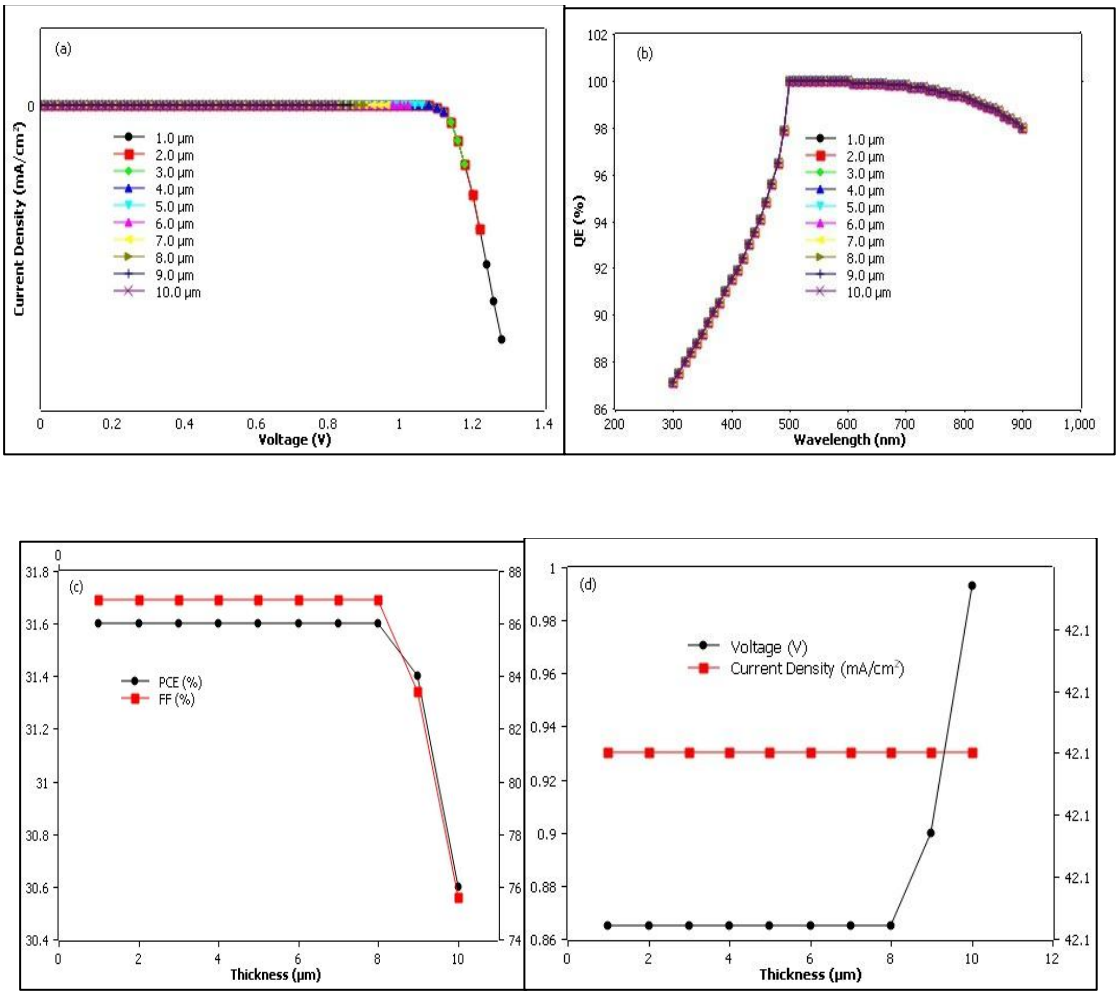

Figure 3.1 (a) J-V curve with at different thickness (b) comparison of QE with Wavelength at different thickness (c) comparison of PC E and FF curve at different thickness (d) comparison of Voc and Jsc Curve at different thickness

Figure 3.2a shows that the thickness of the HTL layer does not affect J-V curve rather the V_{oc} were shut circuited at different J_{sc} with different thickness values which is also observed in QE and wavelength plot. Generally speaking, the selected values for different thickness of the HTL layer does not signifies unique changes in the performance of the PSC device rather, little changes were observed at 8-10 µm which shows a decrease in the PCE and FF as shown in Figure 3.2c, in figure 3.2d an increase in voltage was similarly observed at the same thickness range of 8-10 µm but there was no changes in the current density [17]. The PCE, FF, V_{oc} and J_{sc} performance is at its best from 1-7 µm with values 31.6 %, 86.9 %, 0.86 V and 42.1 mA/cm^2 respectively [18].

3.3 The Influence of HTL Acceptor Density on the Performance PSC

The acceptor density plays a very unique role in the performance of the device structure, it is where the materials are clarified in terms of HTL, ETL and absorber layer [19, 20]. The ETL layer is mostly made up of donors while the Absorber layer contains more of the acceptors to enable effective absorption of solar radiant and enhance flow of charge carriers. The acceptor density was varied with values between (10^{11}-10^{20}) cm^{-3}, the simulation resulted in obtaining values for PCE, FF, V_{oc} and J_{sc} as shown in table 3.2.

Table 3.2 I-V curve simulation data with varying acceptor density

ACCEPTOR DENSITY (CM^{-3})	PCE (%)	FF (%)	V_{OC} (V)	J_{SC} (MA/CM^2)
10^{11}	14.2	76.09	0.865	42.1
10^{12}	16.2	77.90	0.865	42.1
10^{13}	18.1	79.40	0.865	42.1
10^{14}	20.2	81.80	0.865	42.1
10^{15}	22.0	84.50	0.865	42.1
10^{16}	23.1	84.80	0.865	42.1
10^{17}	26.5	85.59	0.865	42.1
10^{18}	30.0	86.40	0.865	42.1
10^{19}	31.6	86.80	0.900	42.1
10^{20}	31.7	86.90	0.993	42.1

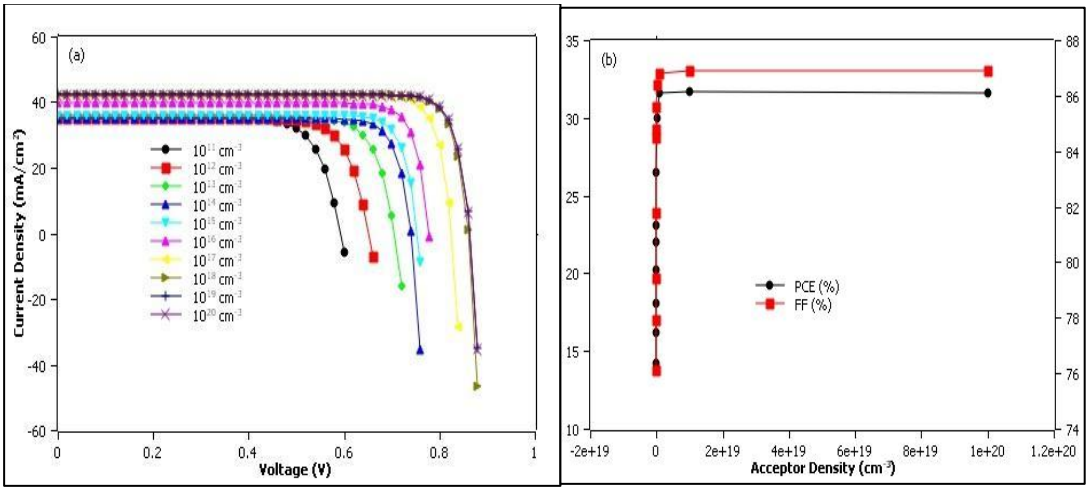

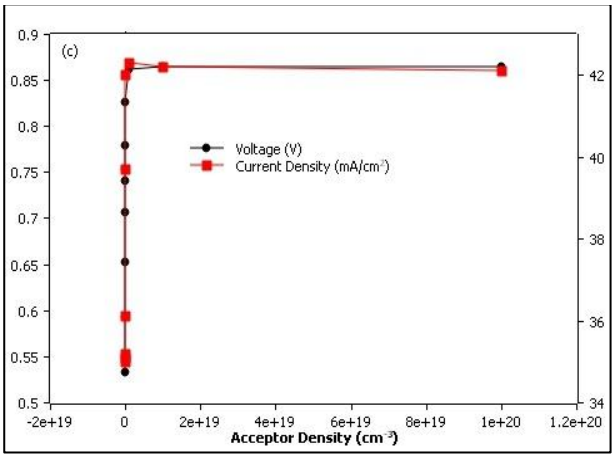

Figure 3.3 (a) J-V curve with different acceptor density values (b) comparison between PCE and FF at different acceptor densities (c) comparison between V_{oc} and J_{sc} at different acceptor densities

Figure 3.3a shows a significant impact of the acceptor density on the current density-voltage properties, the acceptor density increases the PCE values of the device due to an increase in the hole charge careers, the PCE and FF became so high at 10^{19}-10^{20} cm^{-3} with values of 31.6 and 31.7 3%, 86.8 and 89.9 % respectively as shown in figure 3.3b. These values indicate an important shift in the advancement of PCS devices in order to improve its energy generation capacity [21, 22]. These properties were similarly observed in figure 3.3d where the voltage also increases with increase in the acceptor density and reversal for the current density with best values of 0.9 V and 42.1 mA/cm^2. The result obtained shows how effective hole charge careers are to PSC device performances, therefore acceptor density should be taken seriously in order to improve PSC devices.

3.4 The Influence of Absorber Layer Thickness on the Performance of PSC

The absorber layer controls the activities of charge careers with majority holes in a PSC device, it traps and enables the effective flow of the solar radiant for energy generation. Optimizing the properties of the absorber layer will boost the efficiency and performance of the device, this is achievable by ensuring the desirable parameters are fabricated on the device to achieve success [23]. Table 3.3 shows the data generated during the simulation at different thickness with a characteristics graph as shown in figure 3.4. The simulation was carried out at thickness values between 0.1-1 µm and wavelength 300-900 nm with V_{oc} from 0-1 V.

Table 3.3 I-V curve simulation data with varying thickness values

Thickness (μm)	*PCE (%)*	*FF (%)*	*V_{oc} (V)*	*J_{sc} (mA/cm^2)*
0.1	*31.8*	*86.8*	*0.861*	*42.5*
0.2	*17.9*	*86.9*	*0.873*	*23.7*
0.3	*25.1*	*86.9*	*0.876*	*33.0*
0.4	*28.4*	*86.9*	*0.875*	*37.3*
0.5	*30.0*	*86.9*	*0.872*	*39.6*
0.6	*30.8*	*86.9*	*0.870*	*40.8*
0.7	*31.3*	*86.9*	*0.867*	*41.5*
0.8	*31.6*	*86.9*	*0.865*	*42.0*
0.9	*31.7*	*86.9*	*0.863*	*42.3*
1.0	*31.8*	*86.8*	*0.861*	*42.5*

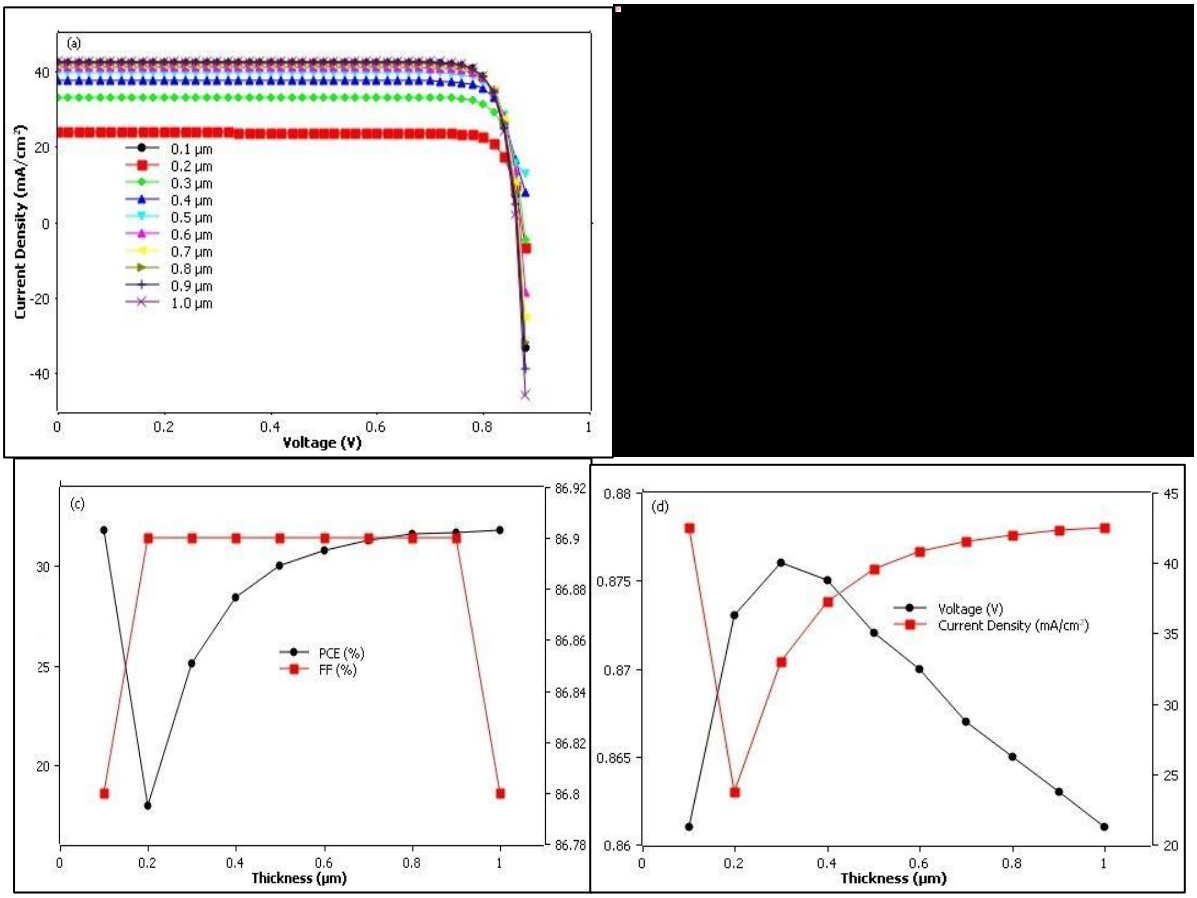

Figure 3.4 (a) J_{sc} and V_{oc} curve at different thickness values (b) QE and wavelength at different thickness values (c) comparison between FF and PCE at different thickness (d) comparison between V_{oc} and J_{sc} at different thickness

The result obtained during this simulation gives a clear effect and how impactful an absorber can be to any PSC device, the thickness changes causes a lot of data alteration and that is a choice of absorber layer thickness is very important in order to maximize the efficiency of the device [24]. In figure 3. 4a&b shows that the thickness parameters affect the current density and decline at a voltage >0.8, similarly observed with the quantum efficiency (QE) where the thickness causes significant changes with QE >80 % and decreases as it approaches 900 nm [25]. The PCE values start to decrease at first then it later increases from 0.5 µm and for the fill factor it increases to from 0.1 µm, it then remains steady at 86.9 % until it was 1 µm then it decreases as shown in figure 3.4c. Considering figure 3.4d, the voltage first decreases at 0.2 µm then increases to the initial voltage value, and the current density also increases and decreases sharply which shares an approximate parallel view with the voltage as presented [26]. The optimal values for PCE, FF, V_{oc} and J_{sc} generated for this optimization includes 32.8 %, 86.9%, 0.861 V and 42.5 mA/cm^2 respectively [27].

3.5 The influence of ETL layer thickness on the performance of PSC.

The effectiveness of the ETL layer determines the efficiency of the absorber layer; the ETL layer has firsthand contact with the solar radiation before it reaches the absorber layer [28]. Good material for the ETL layer and the choice of appropriate parameters will greatly enhance the flow of charge careers into the electrode and boost large energy harvest for PSC. The range of values used to determine thickness effect were 0.1-1 µm, the voltage was set at maximum 1.5 V, and the wavelength between 300-900 µm [29]. nearly similar properties was observed

as seen in absorber layer thickness with a significant effect on the J-V Curve as seen in figure 3.5a where the thickness affect the level of current density, this also directly affect the values of QE at different level due to the increase in wavelength, at 0.2 µm thickness the wavelength shows a unique decrease of QE compared to the rest of the thickness values as shown in figure 3.5b. No dissatisfactory effect of the thickness values was observed on PCE until when it reaches 1.0 Mm then a slide decrease is seen, and for FF it remains the same but slightly decreases at thickness of >0.6 µm [30]. The V_{oc} were the same throughout all the thickness values but a slight decrease was observed at >0.7 µm thickness values [31]. The most appreciated values for these simulation PCE, FF, V_{oc} and J_{sc} are at 31.6 %, 86.9 %, 0.865 V and 4.21 mA/cm^2 respectively. The ETL layer plays a vital role in enabling incident solar radiation to be absorbed by the absorber layer with minimal reflectance and controls the flow of the charge carriers at the electrode.

Table 3.4 J-V simulation data at different thickness values

Thickness (µm)	PCE (%)	FF (%)	V_{oc} (V)	J_{sc} (mA/cm^2)
0.1	31.6	86.9	0.865	42.1
0.2	31.6	86.9	0.865	42.1
0.3	31.6	86.9	0.865	42.1
0.4	31.6	86.9	0.865	42.1
0.5	31.6	86.9	0.865	42.1
0.6	31.6	86.8	0.865	42.1
0.7	31.6	86.8	0.865	42.0
0.8	31.6	86.8	0.865	42.0
0.9	31.6	86.8	0.865	42.0
1.0	31.5	86.8	0.865	42.0

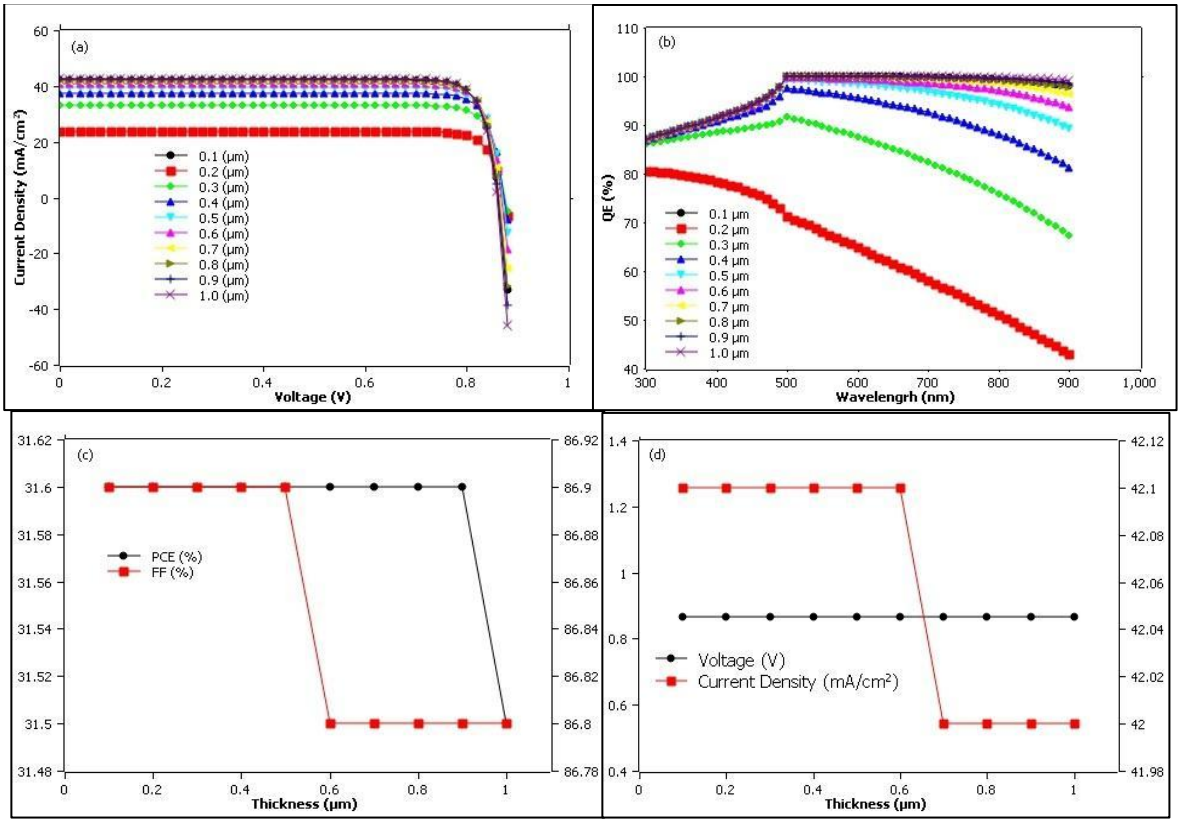

Figure 3.5 (a) J_{sc} and V_{oc} plot at different thickness values (b) QE and wavelength plot at different thickness values (c) comparison between PCE and FF at different thickness (d) comparison of V_{oc} and J_{sc} at different thikness

4. Conclusion

The SCAPS-1D simulation was used in this research to investigate the effective electrical and optical performance of $CsPbI_3$ material in perovskite solar cell (PSC) devices. The initial input of the simulator software was set at 300 K, light spectrum of (1000 Wm^{-2}) AM1_5G 1, wavelength ranging between 300-900 nm, and with a maximum voltage of 1.5 V. Spiro-OMeTAD was used as HTL layer, $CsPbI_3$ absorber layer, TiO_2 as ETL layer and FTO as front contact. The PSC device structure is in the form of Spiro-OMeTAD/$CsPbI_3$/TiO_3/FTO, the numerical investigation was carried out on thickness and acceptor density of the structure in order to obtain a remarkable optimize performance of the device. The initial numerical simulation of the device gives the results of PCE at 31.61 %, FF at 86.88 %, J_{sc} at 42.0857 mA/cm^2 and V_{oc} of 0.865 V. Considering the effect of thickness layer of HTL layer, there was only little adjustment observed at the numerical data but when the acceptor density was investigated a significant increase was observed across the numerical data with good performance at acceptor density $>10^{19}$ cm^{-3}. The effect of results on the ETL layer increases the efficiency of the flow of charge carriers across the electrode, varying the thickness from 0.1-1.0 μm the PCE becomes even more effective at 1.0 μm [32]. The effect of thickness on the ETL layer shows a decrease in PCE and the current density (J_{sc}), but the voltage flows steadily with no changes observed. The thickness of each layer, defect density and interfaces all are vital to ensuring optimal performance of a PSC device therefore, it is important to be deliberate about the choice of each parameter during fabrication of PSC device for energy generation [33].

Acknowledgement

The authors would like to appreciate Professor Marc Burgelman and his counterpart at the department of electronics and information system, university of Gent for the effort they put towards developing the SCAPS software and allowing its usage for better numerical PSC data analysis.

Conflict of Interest

The authors declared no conflict of interest at the course of the research.

Funding

This research did not receive any form of funding external or within the institution of studies.

REFERENCE

[1] S. E. BOUSSAADA, Y. MOUCHAAL , H. RIANE and A. KHELIL, "Deep Insights Into The Coupled Optoelectronic Analysis Of ETL Thin Films And Photovoltaic Analysis Of CsPbI 3 -Based Perovskite Solar Cell Using SCAPS-1D Simulations," Research Square, 2025. https://doi.org/10.21203/rs.3.rs-5883627/v1.

[2] Y. K. Burak and M. A. Ehsan, "Optimization of several parameters towards 30% effeciency perovskite based solar cell using SCAPS 1D software," Iraqi Journal of Physics, vol. 22, pp. 117-129, 2024. https://doi.org/10.30723/ijp.v.22i4.1287.

[3] E. Danladi, M. Kashif, A. Ichoja and B. Ayiya, "Modeling of a Sn-Based HTM-Free Perovskite Solar Cell Using a One-Dimensional Solar Cell Capacitance Simulator Tool," Trans. Tianjin Univ, vol. 29, p. 62–72, 2023. https://doi.org/10.1007/s12209-022-00343-w.

[4] B. M. Soucase, . I. G. Pradas and K. R. Adhikari, "Numerical Simulations on Perovskite Photovoltaic Devices," Intech, vol. 3, pp. 42-54, 2016. https://doi.org/doi.org/10.5772/61751

[5] M. A. Hachim, . A. Tarbi, M. El-Mrabet, H. Erguig and T. Chtouki , "Numerical modeling and DFT study for a CsPbCl3 lead-based perovskite solar cell using Zn-doped Cu2O as HTL," Research Square, 2024. https://doi.org/10.21203/rs.3.rs-4184560/v2

[6] H. Adnan, R. Sabrina, B. Maroua and R. A. Sheikh, "Impact of Hole Transport Layers in Inorganic Lead-Free B--CsSnI3 Perovskite Solar Cells: A Numerical Analysis," Engineering Proceedings, no. 41, pp. 19-30, 2022. https://doi.org/10.3390/ECP2022-12611.

[7] A. A. Goje, Ludin, A. N. Ludin, A. M. Sheriff, W. M. Zanna and M. Isah, "Optimisation of PCBM on Al2O3 Electron Transport Layer for Improved Performance of Perovskite Solar Cells Using SCAPS 1D," Nigerian Institude of Physics, vol. 32(1), 2023.

[8] A. Hosen, S. Rahman, M. Brella and S. R. Al'Ahmed, "Impact of Hole Transport Layers in Inorganic Lead-Free B--CsSnI3 Perovskite Solar Cells: A Numerical Analysis," MDPI Engineering Proceedings, vol. 19, 2022. https://doi.org/10.3390/ECP2022-12611.

[9] E. Danladi, C. U. Achemb, I. O. Echic, S. U. Michael and M. E. Onie, "Thickness Variation Study of Perovskite Layer Over the Range 100 1300 nm and Its Influence on the Performance of Perovskite Solar Cells Using SCAPS Software," Journal of Nano and Materials Science Research, vol. 1, pp. 22-27, 2022.

[10] G. Pindolia, M. S. Shinde and K. P. Jha, "Optimization of an inorganic lead free RbGeI3 based perovskite solar cell by SCAPS-1D simulation," Solar Energy, vol. 236, pp. 802-821, 2022. . https://doi.org/10.1016/j.solener.2022.03.053.

[11] T. N. Gabriel, T. I. Jonathan, G. Federick, M. A. Terwase and D. Eli, "Numerical Analysis of the Absorber Layer of Perovskite Solar Cells based on Cu2O as Hole Transporting Material," Journal of Energy Research and Reviews, vol. 17, no. 1, pp. 52-65, 2025. https://doi.org/10.9734/jenrr/2025/v17i1392.

[12] A. C. Ozurumba, N. V. Ogueke, C. A. Madu, E. Danladi, C. P. Mbachu, A. S. Yusuf, P. M. Gyuk and I. Hossain, "SCAPS-1D simulated

organometallic halide perovskite: A comparison of perfomance under Sub-Saharan temperature condtion," Helion, vol. 10, no. 8, 2024. https://doi.org/10.1016/j.heliyon.2024.e29599.

[13] S. Tuo, K. B. m. Koffi, K. A. Kamenan and J. Datte, "SCAP 1D simulation of a lead-free perovskite photovaltaic solar cell using hematite as electron transport layer," scientific research publishing, vol. 14, pp. 97-106, 2024. https://doi.org/10.4236/mnsms.2024.144006.

[14] E. Danladi, A. Salawu, M. Abdulmalik, E. D. Onoja, E. E. Onwoke and A. D. S, "Optimization of Absorber and ETM Layer Thickness for Enhanced Tin based Perovskite Solar Cell Performance using SCAPS-1D Software," Physics Access, vol. 2, pp. 1-11, 2022. https://doi.org/10.47514/phyaccess.2022.2.1.001.

[15] M. Safdar, X. Yang, Q. Furong and H. Meng, "Investigating the Performance of Efficient and Stable Planer Perovskite Solar Cell with an Effective Inorganic Carrier Transport Layer Using SCAPS-1D Simulation," Energies, vol. 16, pp. 7438-7452, 2023. . https://doi.org/10.3390/en16217438.

[16] A. Rihan, M. Md Masum, H. Md. Faruk, A. Mongi, E. Safa, Z. B. Mutasem and R. Md. Ferdous, "AI-Guided SCAPS-1D Optimization of CH 3 NH 3 PbI 3 /La 2 NiMnO 6 Double Absorber Perovskite Solar Cells Achieving Over 33% Efficiency," Journal of Chemistry, vol. 57, pp. 187-196, 2025. https://doi.org/10.1039/D5NJ03896K.

[17] D. Elif, K. Emre and S. Ayse, "Exploring Efficiency and Design Optimization of Flexible Perovskite Solar Cells using SCAPS-1D Simulation," Eurasian Journal of Science Engineering and Technology, vol. 4, no. 2, pp. 42-049, 2023. https://doi.org/10.55696/ejset.1303146.

[18] I. A. Matthew, S. Y. Abubakar, A. Eghwubare, O. E. Stephen, E. James, M. A. Raymond, C. E. Lilian, U. E. Emmanuel, A. Emmanuel, E. Chinyer, T. Nicholas, O. Anthony and E. Danladi, "SCAPS-1D Analysis of Non-Toxic Lead-Free Masni3 Perovskite-Based Solar Cell Using Inorganic Charge Transport Layers," East European Journal Of Physics., vol. 3, pp. 447-455, 2024. https://doi.org/10.26565/2312-4334-2024-3-54.

[19] M. Usha, V. Victor and T. K, "Simulation and Analysis of Lead based Perovskite Solar Cell using SCAPS-1D," Indian Journal of Science and Technology, vol. 10, no. 11, pp. 34-42, 2017. https://doi.org/10.17485/ijst/2017/v11i10/110721.

[20] D. Phuc Van, T. P. L. Phuong and T. K. Cuc Nguyen, "Simulation and optimization of MoS2 layers in solar cells using SCAPS-1D: a comparative study with experimental results," IOP Science, vol. 100, pp. 1402-4896, 2025. https://doi.org/10.1088/1402-4896/adba1c.

[21] O. A. Muhammed, D. Eli, C. O. Rita, M. G. Philibus, S. M. A. C. E. D. T. Francis U. Salifua, U. S. Francis, M. Suleiman and C. E. Anselem, "Numerical Study of 25.459% Alloyed Inorganic Lead-Free Perovskite Cssngei3-Based Solar Cell by Device Simulation," ResearchGate, pp. 4-12, 2022. https://doi.org/10.26565/2312-4334-2022-4-12.

[22] P. Hyun-Jae, S. Hyojung and J. Byoung-Seong, "SCAPS-1D Simulation for Device Optimization to Improve Efficiency in Lead-Free CsSnI3 Perovskite Solar Cells," MDPI Iorganic, vol. 4, pp. 123-134, 2024. https://doi.org/10.3390/inorganics12040123.

[23] U. Jessica Amuchi, A. O. Joshua, Y. O. Mohammed, D. Eli, M. U. Samuel and R. U. Ugbe, "The Effect of Temperature Dependence on Tin Perovskite Solar Cell Using Scaps 1d," Fudma Journal of Sciences (FJS), Vol. 7, No. 2, Pp. 321 - 329, 2023. https://doi.org/10.33003/fjs-2023-0702-2044.

[24] M. Wahid, M. Howlader, N. Ahasan and M. Rahman, "Performance Improvement of CIGS Solar Cell: A Simulation Approach by SCAPS-1D. Energy and Power engineering," energy and Power Engineering, vol. 15, pp. 291-

306, 2023. https://doi.org/10.4236/epe.2023.158015.

[25] D. Arnob, D. P. Susmita, A. M. A. Md, S. MostafaM, H. Md. Sejan and D. Barun Kumar, “Numerical Simulation and Optimization of Inorganic Lead-Free Cs3Bi2I9-Based Perovskite Photovoltaic Cell: Impact of Various Design Parameters,” Energies, vol. 16, pp. 2328-2332, 2023. https://doi.org/10.3390/en16052328.

[26] S. Abdelhadi, B. Mama and M. Laarej, "Numerical Study of Based Perovskite Solar Cells by SCAPS-1D," International Journal of Energy and Environment , Vol. 13, No. 2308-1007 , Pp. 19-24, 2019.

[27] S. Ullah, F. Khan and F. Rasheed, "Optimizating the Working Mechanism of CsPbI3 Heterojunction Solarells using SCAPS-1D," ScienceDirect, vol. 310, 2024. https://doi.org/10.1016/j.ijleo.2024.171882.

[28] H. Khalid, B. Sagar, A. Arnabc, K. Mustafa, A. Mohammed, P. Rahul, H. A. Md, R. Md. Ferdous, I. Md. Rasidul, Samajdar, M. Jaya and D. Bencherifi, "Harnessing the potential of CsPbBr3-based perovskite solar cells using efficient charge transport materials and global optimization," Royal Chemistry Society, vol. 13, pp. 21044-21062, 2023. https://doi.org/10.1039/D3RA02485G.

[29] D. A. Vívian, F. N. Ana, C. T. Juliana and J. d. S. Leandro, "Advances in lead-free perovskite solar cell design via SCAPS-1D simulations," Royal Society for Chemistry, vol. 4, pp. 4314-4335, 2024. https://doi.org/10.1039/D5SU00526D.

[30] D. Eli, M. G. Philibus, N. T. Nicholas, C. E. Anselem, B. ebidatta, H. Ismail, M. B. Ibrahim, L. M. Mohammad and T. I. Jonathan, "Impact of hole transport material on perovskite solar cells with different metal electrode: A SCAPS-1D simulation insight," Heliyon, pp. 2405-8440, 2023. https://doi.org/10.1016/j.heliyon.2023.e16838.

[31] B. Sujan, D. Arnos, K. D. Barun and I. Nurul, "Numerical simulation and performance optimization of a lead-free inorganic perovskite solar cell using SCAPS-1D," Heliyon, vol. 10, no. 1, pp. 3458-3471, 2021. https://doi.org/10.1016/j.heliyon.2024.e23985.

[32] C. O. Lawani, G. J. Ibeh, O. O. Ige, D. Eli, J. O. Emmanuel, U. A. J and P. O. Oyedare, “Corrigendum to “Numerical Simulation of Copper Indium Gallium Diselenide Solar Cells Using One Dimensional SCAPS. Software,” Journal of the Nigerian Society of Physical Sciences, vol. 3, p. 48–58, 2023. https://doi.org/10.46481/jnsps.2021.133

[33] Q. Chu, W. S, W. Q, C. Z, W. J, L. W, M. S, M. X, C. J and D. J, "Design and performance optimization of carbon-based all-inorganic CsPbIBr2 perovskite battery with C60 buffer layer," Sol. Energy, vol. 246, p. 245–255, 2022. https://doi.org/10.1016/j.solener.2022.10.002.